Kinetics and Thermodynamic Properties of the Thermal Decomposition of Manganese Dihydrogenphosphate Dihydrate

Banjong Boonchom*

King Mongkut's Institute of Technology Ladkrabang, Chumphon Campus, 17/1 M. 6 Pha Thiew District, Chumphon 86160, Thailand

The thermal decomposition of manganese dihydrogenphosphate dihydrate $Mn(H_2PO_4)_2 \cdot 2H_2O$ was investigated in air using differential thermal analysis-thermogravimetry. $Mn(H_2PO_4)_2 \cdot 2H_2O$ decomposes in two steps and the final decomposition product ($Mn_2P_4O_{12}$) was studied by X-ray powder diffraction and FT-IR spectroscopy. The activation energies of the dehydration and decomposition steps of $Mn(H_2PO_4)_2 \cdot 2H_2O$ were calculated through the isoconversional methods of Ozawa and Kissinger−Akahira−Sunose and the possible conversion functions have been estimated through the Coats−Redfern method. The activation energy calculated for the dehydration and decomposition of $Mn(H_2PO_4)_2 \cdot 2H_2O$ by different methods and techniques were found to be consistent. The possible conversion functions of the dehydration and decomposition reactions for $Mn(H_2PO_4)_2 \cdot 2H_2O$ were "cylindrical symmetry" and "three-dimension diffusion", respectively. Activated complex theory has been applied to each step of the reaction and the thermodynamic functions ΔH^*, ΔG^* and ΔS^* are calculated. These values for two stages showed that they are connected with the introduction of heat and are nonspontaneous processes.

1. Introduction

Manganese phosphate compounds are recently gaining more and more interest as materials to be used in the field of catalysis, superphosphate fertilizers, ceramics, and antiproof corrosions.[1–3] They are transformed to other phosphates by hydrolysis and dehydration reactions at elevated temperatures.[4,5] Thermal treatment of manganese phosphates has a great synthetic potential as it may turn simple compounds into advanced materials, which relates to the hydrate in the conventional crystal form.[6,7] Studies on the thermodynamics, mechanisms, and kinetics of solid-state reactions are a challenging and difficult task with complexity resulting from the great variety of factors with diverse effects such as reconstruction of solid state crystal lattices, formation and growth of new crystallization nuclei, diffusion of gaseous reagents or reaction products, materials heat conductance, static or dynamic character of the environment, physical state of the reagents, that is, dispersity, layer thickness, specific area and porosity, type, amount and distribution of the active centers on solid state surface, etc.[8,9] The results obtained from such studies can be directly applied in materials science for the preparation of various metals and alloys, cements, ceramics, glasses, enamels, glazes, and polymer and composite materials.

In this respect, the thermal dehydration and decomposition reactions of $Mn(H_2PO_4)_2 \cdot 2H_2O$ have attracted the interest of kinetics and thermodynamic scientists. The obtained decomposition product is manganese cyclotetraphosphate ($Mn_2P_4O_{12}$), which has interesting inorganic dye pigment, superphosphate fertilizer, and electrochemical properties.[6,7,10] The key factor is that different properties of $Mn_2P_4O_{12}$ depend on different preparative methods, which affect its electrochemical and catalytic performances.[2,3] In the literature, $Mn_2P_4O_{12}$ has been prepared by hydrothermal or high temperature (573 K to 773 K) methods over a long time period (20 h).[11]

The aim of the present paper is to study the kinetic and thermodynamic parameters of the formation of $Mn_2P_4O_{12}$ from the decomposition of $Mn(H_2PO_4)_2 \cdot 2H_2O$ and is followed using differential thermal analysis-thermogravimetry (TG-DTG/DTA), X-ray powder diffraction (XRD), and Fourier Transform-infrared (FTIR) spectroscopy. Nonisothermal kinetics results in two decomposition steps of $Mn(H_2PO_4)_2 \cdot 2H_2O$ that were interpreted using the isoconversional methods of Ozawa[12] and Kissinger−Akahira−Sunose (KAS)[13] and the possible conversion functions have been estimated through the Coats−Redfern method.[14] The thermodynamic (ΔH^*, ΔS^*, ΔG^*) and kinetic (*E, A,* mechanism, and model) parameters of the decomposition reactions of $Mn(H_2PO_4)_2 \cdot 2H_2O$ are discussed for the first time.

2. Experimental Section

$Mn(H_2PO_4)_2 \cdot 2H_2O$ was prepared according to previous work.[15] Thermal analysis measurements (thermogravimetry (TG), differential thermogravimetry (DTG), and differential thermal analysis (DTA)) were carried out by a Pyris Diamond Perkin-Elmer apparatus by increasing the temperature from (303 to 573) K with calcined α-Al_2O_3 powder as the standard reference. The experiments were performed in static air at heating rates of (5, 10, 15, and 20) K min^{-1}. The sample mass was between 6.0−10.0 mg and placed into an alumina crucible without pressing. The structure of the prepared product and the calcined sample were studied by X-ray powder diffraction using a D8 Advanced powder diffractometer (Bruker AXS, Karlsruhe, Germany) with Cu Kα radiation (λ = 0.15406 Å). The room temperature FTIR spectra were recorded in the range of (4000 to 370) cm^{-1} with 8 scans on a Perkin-Elmer Spectrum GX FT-IR/FT-Raman spectrometer with a resolution of 4 cm^{-1} using KBr pellets (spectroscopy grade, Merck).

* Corresponding author. Tel: +66-7750-6422, ext. 4565. Fax: +66-7750-6410. E-mail: kbbanjon@kmitl.ac.th.

10.1021/je800103w CCC: $40.75
Published on Web 06/05/2008

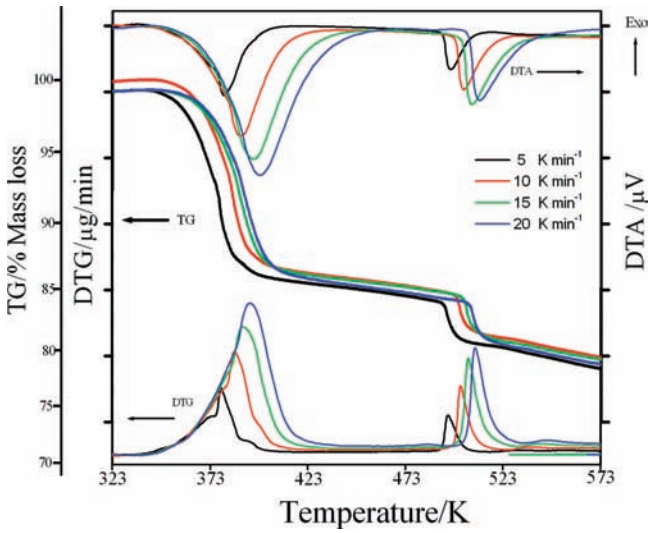

Figure 1. TG-DTG/DTA curves of $Mn(H_2PO_4)_2 \cdot 2H_2O$ in air at four heating rates ((5, 10, 15 and 20) K min^{-1}).

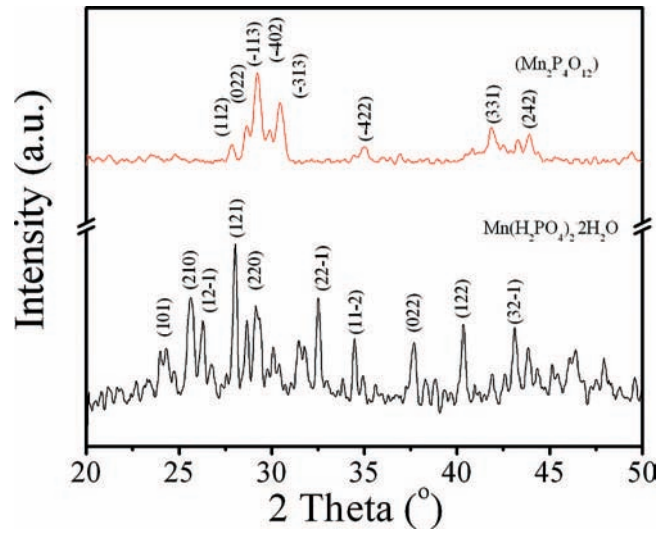

Figure 2. The XRD patterns of $Mn(H_2PO_4)_2 \cdot 2H_2O$ and its dehydration product ($Mn_2P_4O_{12}$).

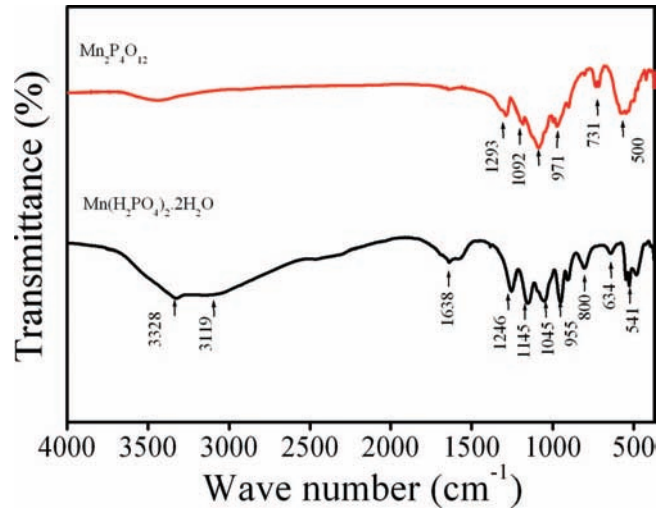

Figure 3. FTIR spectra of $Mn(H_2PO_4)_2 \cdot 2H_2O$ and its dehydration product ($Mn_2P_4O_{12}$).

3. Results and Discussion

3.1. Sample Characterization. TG-DTG/DTA curves of the thermal decomposition of $Mn(H_2PO_4)_2 \cdot 2H_2O$ at four heating rates are shown in Figure 1. All curves are approximately the same shape and indicate that the mass loss is independent of the heating rate. All TG curves of $Mn(H_2PO_4)_2 \cdot 2H_2O$ show two well-defined stages of mass loss in the range of (323 to 573) K, which are related to the elimination of water molecules and phase transformation. The total mass loss is 21.30 % (3.40 mol H_2O), which is close to the theoretical value (25 %, 4 mol H_2O). The retained mass is about 78.70 % for all heating rates, compatible with the value expected for the formation of $Mn_2P_4O_{12}$, which was verified by XRD measurement. The two peaks in the DTG and DTA curves closely correspond to the mass loss observed on the TG trace. Additionally, two decomposition steps were shifted toward higher temperatures when the heating rates increase. The decomposition reactions of $Mn(H_2PO_4)_2 \cdot 2H_2O$ are complex processes, which involve the dehydration of the coordinated water molecules (2 mol H_2O) and an intramolecular dehydration of the protonated phosphate groups (2 mol H_2O) as shown in equations (1) and (2):

$$Mn(H_2PO_4)_2 \cdot 2H_2O \rightarrow Mn(H_2PO_4)_2 + 2H_2O \quad (1)$$

$$Mn(H_2PO_4)_2 \rightarrow 1/2Mn_2P_4O_{12} + 2H_2O \quad (2)$$

An intermediate compound (acid polyphosphate, $Mn(H_2PO_4)_2$) has been registered. Manganese cyclotetraphosphate $Mn_2P_4O_{12}$ was found to be the product of the thermal decomposition at $T > 550$ K. To gain the complete decomposition of $Mn(H_2PO_4)_2 \cdot 2H_2O$, a sample of $Mn(H_2PO_4)_2 \cdot 2H_2O$ was heated in a furnace at 573 K for 2 h.

The XRD patterns of $Mn(H_2PO_4)_2 \cdot 2H_2O$ and its dehydration product ($Mn_2P_4O_{12}$) are shown in Figure 2. All detectable peaks are indexed as the $Mn(H_2PO_4)_2 \cdot 2H_2O$ and $Mn_2P_4O_{12}$ compounds with structure in standard data as PDF # 350010 and PDF # 380314, respectively. These results indicated that the two crystal structures are in the monoclinic system with space group $P2_1/n$ ($Z = 2$) for $Mn(H_2PO_4)_2 \cdot 2H_2O$ and $C2/c$ ($Z = 4$) for $Mn_2P_4O_{12}$.[15]

FTIR spectra of $Mn(H_2PO_4)_2 \cdot 2H_2O$ and its dehydration product ($Mn_2P_4O_{12}$) are shown in Figure 3. Vibrational bands are identified in relation to the crystal structure in terms of the fundamental vibrating units namely $H_2PO_4^-$ and H_2O for $Mn(H_2PO_4)_2 \cdot 2H_2O$ and the $[P_4O_{12}]^{4-}$ ion for $Mn_2P_4O_{12}$, which are assigned according to the literature.[16,17] Vibrational bands of $H_2PO_4^-$ ion are observed in the regions of (300 to 500, 700 to 900, 1160 to 900, 840 to 930, 1000 to 1200 and 2400 to 3300) cm^{-1}. These bands are assigned to the $\delta(O_2PO_2)$, γ(POH), δ(POH), $\nu(PO_2(H_2))$, $\nu(PO_2)$, and ν(OH) vibrations, respectively. The observed bands in the 1600 to 1700 cm^{-1} and 3000 to 3500 cm^{-1} regions are attributed to the water bending/C band and stretching vibrations/A band, respectively. Vibrational bands of the $[P_4O_{12}]^{4-}$ ion are observed in the ranges (1350 to 1220, 1150 to 1100, 1080 to 950, and 780 to 400) cm^{-1}. These bands can be assigned to the $\nu_{as}(OPO^-)$, $\nu_s(OPO^-)$, ν_{as}(POP), and ν_s(POP) vibrations, respectively.[17,18] The observation of a strong ν_s(POP) band is known to be the most striking feature of the cyclotetraphosphate spectra, along with the presence of the $\nu_{as}(OPO^-)$ band.[18]

3.2. Kinetic Studies. Dehydration of crystal hydrates is a solid-state process of the following type:[19–23] A (solid) → B (solid) + C (gas). The kinetics of such reactions is described by various equations taking into account the special features of their mechanisms. This is a model-free method, which involves measuring the temperatures corresponding to fixed values of α (extent of conversion, $\alpha = m_i - m_t/m_i - m_f$,

Table 1. α−T Data Were Corrected from TG Curves at Different Heating Rates (K min^{-1}) for the First Dehydration Step of $Mn(H_2PO_2)_4 \cdot 2H_2O$

	temperature from TG curves at four heating rages/K							
	the first dehydration step				the second decomposition step			
α	5	10	15	20	5	10	15	20
0.1	359.40	364.36	369.42	371.49	493.25	499.50	502.97	506.69
0.2	365.56	370.40	375.77	378.11	493.89	500.12	503.88	507.25
0.3	369.39	374.65	380.71	382.97	494.39	500.66	504.65	507.79
0.4	372.64	377.61	383.82	387.01	495.17	501.29	505.13	508.43
0.5	375.84	380.59	387.22	389.93	495.86	502.10	505.70	509.22
0.6	377.88	383.09	389.44	392.13	496.90	503.08	507.14	510.16
0.7	379.49	384.47	391.92	394.56	497.74	504.18	508.80	512.33
0.8	381.82	386.36	394.69	397.24	499.55	506.60	511.54	514.70
0.9	386.56	388.11	398.75	402.61	503.29	511.55	517.13	519.61

where m_i, m_f, and m_t are the initial, final, and current sample mass, respectively, at moment t) from experiments at different heating rates (β). The activation energy (E_α) can be calculated according to isoconversional methods. In the kinetic study of $Mn(H_2PO_4)_2 \cdot 2H_2O$, the Ozawa[12] and KAS[13] equations were used to determine the activation energy of the dehydration (first step) and decomposition (second step) reactions.

Ozawa equation:

$$\log \beta = \log\left(\frac{AE_\alpha}{Rg(\alpha)}\right) - 2.315 - 0.4567\left(\frac{E_\alpha}{RT}\right) \quad (3)$$

KAS equation:

$$\ln\left(\frac{\beta}{T^2}\right) = \ln\left(\frac{AE_\alpha}{Rg(\alpha)}\right) - \left(\frac{E_\alpha}{RT}\right) \quad (4)$$

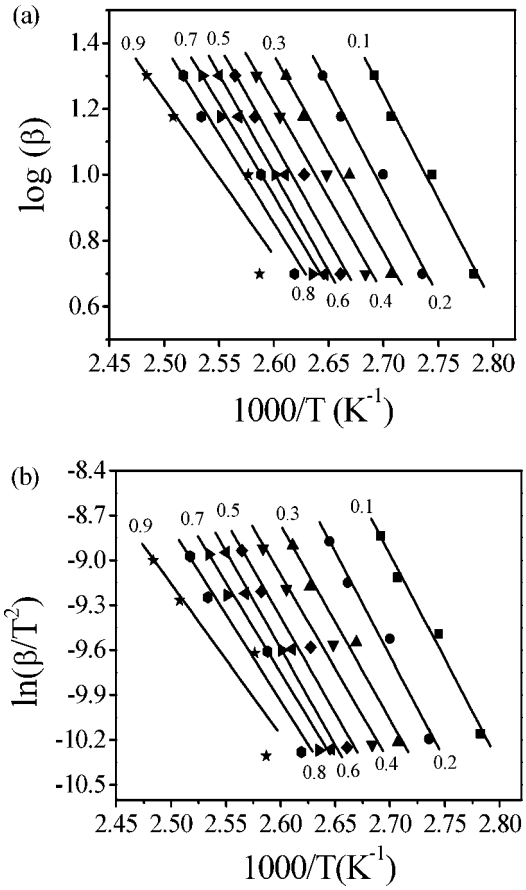

Figure 4. Ozawa (a) and KAS (b) analysis of the first decomposition step of $Mn(H_2PO_4)_2 \cdot 2H_2O$.

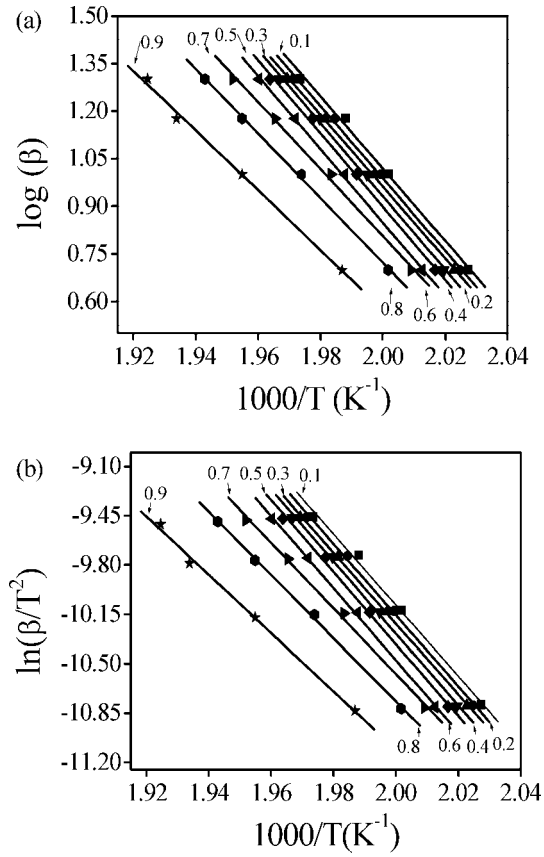

Figure 5. Ozawa (a) and KAS (b) analysis of the second decomposition step of $Mn(H_2PO_4)_2 \cdot 2H_2O$.

where A (the pre-exponential factor/min^{-1}) and E (the activation energy/kJ mol^{-1}) are the Arrhenius parameters, and R is the gas constant (8.314 J mol^{-1}·K^{-1}). The Arrhenius parameters, together with the reaction model, are sometimes called the kinetic triplet. $g(\alpha) = \int_0^\alpha d\alpha/f(\alpha)$ is the integral form of $f(\alpha)$, which is the conversion function for a solid-state reaction and depends on the reaction mechanism.

At the constant condition of others parameters, the TG curves for dehydration and decomposition of $Mn(H_2PO_4)_2 \cdot 2H_2O$ in air at various heating rates ((5, 10, 15, and 20) K min^{-1}) are shown in Figure 1. According to isoconversional methods, the basic data of α and T collected from Figure 1 are illustrated in Table 1. According to eqs 3 and 4, the plots of log β versus 1000/T (Ozawa) and ln β/T^2 versus 1000/T (KAS) corresponding to different conversions α can be obtained by a linear regression using the least-squares method. The Ozawa and KAS analysis results of four TG measurements above 323 K are presented in Figures 4 and 5, respectively. The activation energies E_α can be calculated from the slopes of the straight lines with good coefficient of determination (r^2) values. The slopes change depending on the degree of conversion (α) for the dehydration and decomposition reactions of $Mn(H_2PO_4)_2 \cdot 2H_2O$. The activation energies are calculated at heating rates of (5, 10, 15, and 20) K min^{-1} via the Ozawa and KAS methods in the α range of 0.1 to 0.9. The activation energy values of two decomposition steps calculated by the KAS method are close to those obtained by the Ozawa method (the biggest difference is only about 2.10 kJ mol^{-1}) thus leading to credible results, which are shown in Table 2. If E_α values are independent of α, the decomposition may be a simple reaction,[20,21] while the dependence of E on α should be interpreted in terms of multistep reaction mechanisms.[20,23] The activation energies worked out through the

Table 2. Activation Energies (E_α) and Coefficient of Determination (r^2) Calculated by the Ozawa and KAS Methods on the Basis of the Experimental TG Curves of the First Dehydration and the Second Decomposition Steps of $Mn(H_2PO_2)_4 \cdot 2H_2O$

	the first dehydration step				the second decomposition step			
	Ozawa method		KAS method		Ozawa method		KAS method	
α	E_α kJ·mol^{-1}	r^2	E_α kJ·mol^{-1}	r^2	E_α kJ mol^{-1}	r^2	E_α kJ·mol^{-1}	r^2
0.1	116.45	0.9938	116.39	0.9931	207.16	0.9977	209.54	0.9975
0.2	115.92	0.9916	115.72	0.9906	207.61	0.9990	210.01	0.9989
0.3	108.63	0.9906	107.98	0.9894	206.13	0.9995	208.44	0.9995
0.4	105.54	0.9872	104.68	0.9856	209.77	0.9990	212.26	0.9989
0.5	107.42	0.9841	106.60	0.9821	209.94	0.9985	212.42	0.9984
0.6	108.62	0.9888	107.82	0.9874	209.88	0.9995	212.34	0.9995
0.7	101.36	0.9817	100.15	0.9793	191.82	0.9983	193.33	0.9982
0.8	97.82	0.9731	96.39	0.9695	184.93	0.9995	186.04	0.9994
0.9	85.99	0.9180	83.87	0.9065	171.32	0.9982	171.66	0.9980
Avg[a]	105.31 ± 9.41	0.9853	104.40 ± 10.03	0.9834	199.84 ± 13.94	0.9988	201.78 ± 14.72	0.9987

[a] Avg, average value.

Ozawa and KAS methods for the dehydration and decomposition steps of $Mn(H_2PO_4)_2 \cdot 2H_2O$ vary slightly and the activation energies on the different α approximately give rise to a single master straight line, so we draw conclusion that the two decomposition reactions may be two single kinetic mechanisms.[19,20] The activation energy for the release of the water of crystallization lies in the range of 50 to 130 kJ mol^{-1}, while the values for coordinately bounded decomposition are higher than this range.[20–23] In addition, the water eliminated at 423 K and below can be considered as water of crystallization, whereas water eliminated at 473 K and above indicates its co-ordination by the metal atom.[20–23] The calculated activation energies from the Ozawa and KAS methods for the two dehydration reactions suggest that the water molecules are the water of crystallization and coordinate water for the first and the second steps, respectively. These results are consistent with two endothermic peaks at (389 and 503) K in the DTA curve, respectively.

For the first and second steps, the estimation of kinetic parameters can be turned into a multiple linear regression problem through the Coats−Redfern model.[14]

$$\ln\left(\frac{g(\alpha)}{T^2}\right) = \ln\left(\frac{AR}{\beta E_\alpha}\left[1 - \frac{2RT}{E_\alpha}\right]\right) - \left(\frac{E_\alpha}{RT}\right) \qquad (5)$$

Hence, ln $(g(\alpha)/T^2)$ calculated for the different α values at the single β value on $1/T$ must give rise to a single master straight line, so the activation energy and the pre-exponential factor can be calculated from the slope and intercept through ordinary least-squares estimation. The activation energy, pre-exponential factor and the correlation coefficient can be calculated thought the equation of the Coats−Redfern method combined with 35 conversion functions.[19,21,23] The most probable mechanism function was assumed to be the one for which the value of the correlation coefficient was highest and the activation energies calculated by the Coats−Redfern method were close to the optimized values from the Ozawa and KAS methods.

From the above analysis, the possible conversion function of the dehydration reaction is $F_{1/2}$ (power law model), which has a higher coefficient of determination ($r^2 = 0.99908$) than another functions. Thus, it can be stated that the mechanism function with integral $g(\alpha) = [1 - (1 - \alpha)^{1/2}]$ and differential form $f(\alpha) = 2(1 - \alpha)^{1/2}$ belongs to the mechanism of phase boundary reaction (cylindrical symmetry). The correlated kinetic parameters are $E_\alpha = (107.89 \pm 6.58)$ kJ mol^{-1} and $A = (1.47 \times 10^7 \pm 18.41)$ s^{-1}. Concerning the second step of decomposition, the better coefficient of determination ($r^2 = 0.99546$) was obtained with mechanism function D_5 (Zhuravlev, Lesokin, Tempelman equation), which corresponds to three-dimensional diffusion with integral $g(\alpha) = [(1 - \alpha) - 1]^2$ and differential form $f(\alpha) = (3/2)(1 - \alpha)^{4/3}((1- \alpha)^{-1/3} - 1)^{-1}$. The correlated kinetic parameters are $E_\alpha = (283.06 \pm 36.89)$ kJ mol^{-1} and $A = (6.42 \cdot 10^{21} \pm 2.34 \cdot 10^4)$ s^{-1}. The optimized mechanism functions of the two dehydration processes are different. These are explained as due to the difference between the true scheme decomposition of manganese dihyrdogenphosphate dihydrate (eqs 1 and 2). The first dehydration step involves water of crystallization (2 mol H_2O), which corresponds to phase boundary limited process of cylindrical symmetry $F_{1/2}$ (eq 1), whereas the second step involves intramolecular dehydration of the protonated dihydrogenphosphate groups (2 mol H_2O), which corresponds to the diffusion limited process of the decomposition of $Mn(H_2PO_4)_2$ (eq. 2).

The pre-exponential factor (A) values in the Arrhenius equation for solid phase reactions are expected to be over a wide range (6 or 7 orders of magnitude), even after the effect of surface area is taken into account.[8,24,25] The low factors will often indicate a surface reaction, but if the reactions are not dependent on surface area, the low factor may indicate a "tight" complex. The high factors will usually indicate a "loose" complex.[24] Even higher factors (after correction for surface area) can be obtained for complexes having free translation on the surface. Because the concentrations in solids are not controllable in many cases, it would have been convenient if the magnitude of the pre-exponential factor indicated reaction molecularity. On the basis of these reasons, the first and second steps of the thermal decomposition of $Mn(H_2PO_4)_2 \cdot 2H_2O$ may be interpreted as tight and loose complexes, respectively. The last step exhibits higher activation energy and pre-exponential factor (A) in comparison with the first step, and this is understandable because this step corresponds to a true P−OH bond breaking in connection with polycondensation reaction.[4,7,16] These results are consistent with thermal analysis, which confirms that decomposition product as manganese cyclotetraphosphate ($Mn_2P_4O_{12}$).

From the activated complex theory (transition state) of Eyring,[8,9,24,25] the following general equation may be written

$$A = \left(\frac{e\chi k_B T_p}{h}\right)\exp\left(\frac{\Delta S^*}{R}\right) \qquad (6)$$

where $e = 2.7183$ is the Neper number, χ is the transition factor, which is unity for monomolecular reactions, k_B is the Boltzmann constant, h is Plank's constant, and T_p is the peak temperature of the DTA curve. The change of the entropy may be calculated according to the formula

$$\Delta S^* = R \ln\left(\frac{Ah}{e\chi k_B T_p}\right) \quad (7)$$

Because

$$\Delta H^* = E^* - RT_p \quad (8)$$

when E^* is the activation energy E_a of the Coats−Redfern method. The changes of the enthalpy ΔH^* and Gibbs free energy ΔG^* for the activated complex formation from the reagent can be calculated using the well-known thermodynamic equation

$$\Delta G^* = \Delta H^* - T_p \Delta S^* \quad (9)$$

The heat of activation (ΔH^*), entropy of activation (ΔS^*), and free energy of activation decomposition (ΔG^*) were calculated at $T = T_p$ (T_p is the DTA peak temperature at the corresponding stage in the highest heating rate), because this temperature characterizes the highest rate of the process and therefore is its most important parameter.

As can be seen from Table 3, the entropy of activation (ΔS^*) values for the first and second steps are negative. It means that the corresponding activated complexes had a higher degree of arrangement than the initial state. Because the decomposition of $Mn(H_2PO_4)_2 \cdot 2H_2O$ proceeds as two consecutive reactions, the formation of the second activated complex passed in situ. Obviously, the entropy of the second activated complex was lower than that of the preceding one but they are nearly the same. In the terms of the activated complex theory (transition theory),[8,9,24,25] a positive value of ΔS^* indicates a malleable activated complex that leads to a large number of degrees of freedom of rotation and vibration. A result may be interpreted as a "fast" stage. On the other hand, a negative value of ΔS^* indicates a highly ordered activated complex and the degrees of freedom of rotation as well as of vibration are less than they are in the nonactivated complex. These results may indicate a "slow" stage.[24] Therefore, the first and second steps of the thermal decomposition of $Mn(H_2PO_4)_2 \cdot 2H_2O$ may be interpreted as slow stages. The positive values of the enthalpy ΔH^* are in good agreement with two endothermic effects in DTA data. The positive values of ΔH^* and ΔG^* for all stages show that they are connected with the introduction of heat and they are nonspontaneous processes.

4. Conclusions

$Mn(H_2PO_4)_2 \cdot 2H_2O$ decomposes in two steps by starting after 323 K and the final product is $Mn_2P_4O_{12}$. The decomposition of $Mn(H_2PO_4)_2 \cdot 2H_2O$ is important for its further treatment. The final product was confirmed by XRD and FTIR measurements. The kinetics of the thermal decomposition of $Mn(H_2PO_4)_2 \cdot 2H_2O$ was studied using nonisothermal TG applying model-fitting method. The activation energy calculated for the two decomposition steps of $Mn(H_2PO_4)_2 \cdot 2H_2O$ by different methods and techniques were found to be consistent. This indicates that the activation energy of decomposition is independent of process and the nature of nonisothermal methods as well as TGA. On the basis of correctly established values of the apparent activation energy, pre-exponential factor and the changes of entropy, enthalpy, and Gibbs free energy, certain conclusions can be made concerning the mechanisms and characteristics of the processes. Thus, various scientific and practical problems involving the participation of solid phases can be solved.

Table 3. Values of ΔS^*, ΔH^* and ΔG^* for Two Decomposition Steps of $Mn(H_2PO_2)_4 \cdot 2H_2O$

parameter	the first dehydration step	the second decomposition step
ΔS^* (J mol^{-1} K^{-1})	−231.32	−224.34
ΔH^* (kJ mol^{-1})	104.96	279.19
ΔG^* (kJ mol^{-1})	186.61	383.52

Acknowledgment

The author would like to thank the Department of Chemistry, Khon Kaen University for providing TG-DTG/DTA facilities.

Literature Cited

(1) Kaplanová, M.; Trojan, M.; Brandová, D.; Navrátil, J. On the luminescence on manganese(II) phosphates. *J. Luminescence* **1984**, *29*, 199.
(2) Wang, C.-M.; Liau, H.-C.; Tsai, W.-T. Effect of heat treatment on the microstructure and electrochemical behavior of manganese phosphate coating. *Mater. Chem. Phys.* **2007**, *102*, 207.
(3) Wang, C.-M.; Liau, H.-C.; Tsai, W.-T. Effects of temperature and applied potential on the microstructure and electrochemical behavior of manganese phosphate coating. *Surf. Coat. Technol.* **2006**, *201*, 2994.
(4) Koleva, V.; Mehandjiev, D. Characterization of $M(H_2PO_4)_2 \cdot 2H_2O$ (M = Mn, Co, Ni) and their in situ thermal decomposition by magnetic measurements. *Mater. Res. Bull.* **2006**, *41*, 469.
(5) Assaaoudi, H.; Butler, I. S.; Kozinski, J. A. Crystal structure, vibrational spectra, and thermal decomposition and nitrogen adsorption behaviour of a new tetramanganese(II) dipyrophosphate decahydrate, $Mn_4(P_2O_7)_2 \cdot 10H_2O$. *J. Chem. Cryst.* **2006**, *36*, 723.
(6) Trojan, M.; Brandová, D. A study of thermal preparation OF c-$Mn_2P_4O_{12}$. *J. Therm. Anal. Calorim.* **1985**, *30*, 159.
(7) Antraptseva, N. M.; Shchegrov, L. N.; Ponomareva, I. G. Thermolysis features of manganese(II) and zinc dihydrogenphosphate solid solution. *Russ. J. Inorg. Chem.* **2006**, *51*, 1493.
(8) Ŝesták, J. *Thermodynamical Properties of Solids*; Academia: Prague, 1984.
(9) Young, D. *Decomposition of Solids*; Pergamon Press: Oxford, 1966.
(10) Danvirutai, C.; Boonchom, B.; Youngme, S. Nanocrystalline manganese dihydrogen phosphate dihydrate $Mn(H_2PO_4)_2 \cdot 2H_2O$ and its decomposition product ($Mn_2P_4O_{12}$) obtained by simple precipitation route*J. Alloys Compd.*, in press.
(11) Bagieu-Beucher, M.; Gondrand, M.; Perroux, M. Etude à haute pression des tétramétaphosphates du type $M_2P_4O_{12}$ (M = Ni, Mg, Cu, Co, Fe, Mn, Cd). Données cristallographiques sur tous les composés $M_2P_4O_{12}$. *J. Solid State Chem.* **1976**, *19*, 353.
(12) Ozawa, T. A New Method of Analyzing Thermogravimetric Data. *Bull. Chem. Soc. Jpn.* **1965**, *38*, 1881.
(13) Kissinger, H. E. Reaction Kinetics in Differential Thermal Analysis. *Anal. Chem.* **1957**, *29*, 1702.
(14) Coats, A. W.; Redfern, J. P. Kinetic Parameters from Thermogravimetric Data. *Nature.* **1964**, *20*, 68.
(15) Boonchom, B.; Maensiri, S.; Danvirutai, C. Soft solution synthesis, non-isothermal decomposition kinetics and characterization of manganese dihydrogen phosphate dihydrate $Mn(H_2PO_4)_2 \cdot 2H_2O$ and its thermal transformation products. *Mater. Chem. Phys.* **2008**, *109*, 404.
(16) Koleva, V.; Effenberger, H. Crystal chemistry of $M[PO_2(OH)_2]_2 \cdot 2H_2O$ compounds (M = Mg, Mn, Fe, Co, Ni, Zn, Cd): Structural investigation of the Ni, Zn and Cd salts. *J. Solid State Chem.* **2007**, *180*, 966, and references therein.
(17) Ramakrishnan, V.; Aruldhas, G.; Bigotto, A. Vibrational spectra of Cu(II) and Co(II) tetrametaphosphates. *Infrared Phys.* **1985**, *25*, 665.
(18) Soumhi, E. H.; Saadoune, I.; Driss, A. A New Organic-Cation Cyclotetraphosphate $C_{10}H_{28}N_4P_4O_{12} \cdot 4H_2O$: Crystal Structure, Thermal Analysis, and Vibrational Spectra. *J. Solid State Chem.* **2001**, *156*, 364.
(19) Vlaev, L. T.; Nikolova, M. M.; Gospodinov, G. G. Non-Isothermal Kinetics of Dehydration of Some Selenite Hexahydrates. *J. Solid State Chem.* **2004**, *177*, 2663.
(20) Zhang, K.; Hong, J.; Cao, G.; Zhan, D.; Tao, Y.; Cong, C. The Kinetics of Thermal Dehydration of Copper(II) Acetate Monohydrate in Air. *Thermochim. Acta* **2005**, *437*, 145.
(21) Gao, X.; Dollimore, D. A Kinetic study of The Thermal Decomposition of Manganese (II) Oxalate Dehydrate. *Thermochim. Acta* **1993**, *215*, 47.
(22) Vlase, T.; Vlase, G.; Doca, M.; Doca, N. Specificity of Decomposition of Solids in Non-Isothermal Conditions. *J. Therm. Anal. Calorim.* **2003**, *72*, 597.

(23) Gabal, M. A. Kinetics of the thermal decomposition of $CuC_2O-ZnC_2O_4$ mixture in air. *Thermochim. Acta* **2003**, *402*, 199.
(24) Cordes, H. M. Preexponential factors for solid-state thermal decomposition. *J. Phys. Chem.* **1968**, *72*, 2185.
(25) Criado, J. M.; Pérez-Maqueda, L. A.; Sánchez-Jiménez, P. E. Dependence of the preexponential factor on temperature. *J. Therm. Anal. Calorim.* **2005**, *82*, 671.

Received for review February 11, 2008. Accepted April 21, 2008. This work is financially supported by King Mongkut's Institute of Technology Ladkrabang Research (KMITL Reseach), Ministry of Education, Thailand.

JE800103W